SYNERUPTIVE RHEOLOGICAL PARAMETERS OF STROMBOLI BASALT AND ARENAL ANDESITE: INFERENCE ON THEIR ERUPTIVE DYNAMICS

SARA BERTOLINO
Dipartimento di Scienze Mineralogiche e Petrologiche, Università di Torino, Via Valperga Caluso 35, I-10125 Torino

INTRODUCTION

The aim of this research is the study of the rheological parameters of two open-system volcanoes (Stromboli, Aeolian Islands and Arenal, Costa Rica) which exhibit both strombolian activity. This can be achieved in the light of Crystal Size Distribution (CSD) and experimental research on both natural and experimental analogues; existing rheological models (the so called modified Einstein-Roscoe equations); integration of model and general application for future modeling.

Bulk chemical (XRF) analyses were done in Zurich (Switzerland) at the Institute of Mineralogy and Petrology (IMP-ETH, Swiss Federal Institute of Technology) by means of a wave-length dispersive X-ray fluorescence spectrometer (WD-XRF, Axios, PANalytical), equipped with 5 diffraction crystals. Interstitial glass composition has been determined with a Cambridge SEM- EDS at the University of Turin (Department of Mineralogical and Petrological Sciences). CSD data were collected by means of digital images of thin sections acquired by a JVC-3CCD camera applied to an Olympus BX60 optical microscope, additional binary images of microlites were also obtained from images collected with an EDS microanalyser linked to a Cambridge stereoscan 360 SEM. Images were then analyzed by means of the computer code SCION IMAGE (Scion Corporation, Frederick, Maryland). Crystallization experiments and the experimental measurements of viscosity have been done in Zurich at the Institute of Mineralogy and Petrology (IMP-ETH, Swiss Federal Institute of Technology) by means of a Boyd and England Piston Cylinder apparatus. Viscosity has been calculated applying the new "modified" Tammann-Vogel-Fulcher equation proposed in this work.

GEOLOGICAL BACKGROUND, VOLCANIC ACTIVITY AND ROCK COMPOSITIONS

Stromboli volcano is the only island of the Aeolian Arc which has been in permanent activity in the last 2000 years. Because of its frequent mild explosive activity, it has been taken as a reference case to identify minor to intermediate volcanic eruptions (Newhall & Self, 1982). This type of explosive activity is characterized by an open-conduit system, with explosive events that occur at rather regular intervals of 10-20 minutes with the ejection of scoriae, lapilli, bombs accompanied by an emission of gasses (H_2O, CO_2, SO_2 and in lower contents HCl and HF) from the crater area. This mild activity is periodically interrupted by major eruptive events, such as lava flows (each 4-5 years), and/or major explosions or paroxysms often coeval with the generation of tsunamis (Barberi *et al.*, 1993).

In this study 25 samples were selected as representative, in particular I drawn my attention to lava flows sampled in December 2002, February and June 2003; to scorias and bombs of the "normal" present-day activity sampled in June, November and December 2002; to the so called "Biondo" pumice ejected during the paroxysms occurred on April 5, 2003. Petrochemically, current lavas and tephra are high-K calc-alkaline basalts straddling the shoshonite field. Lavas erupted in 2002-2003 and crystal-rich scorias are characterized by a high degree of crystallinity (from 35 to 45 vol.%) and variable bubble content

(10 to 30 vol.%). They show an identical mineralogy and exhibit a porphyric and seriate texture consisting of plagioclase (bytownite-labradorite), clinopyroxene (augite-diopside) and olivine (Fo_{70}) as phenocrystic phases. Groundmass (30-37 vol.%) appears to be microcrystalline with the same phase assemblages coexisting with a brownish glass. Accessory minerals are Ti-magnetite and apatite. The crystal-poor pumices show a nearly aphyric texture and a low crystallinity content (~ 5 vol.%). Mineral phases are microphenocrysts of plagioclase, clinopyroxene and olivine in a hyaline groundmass (Table 1).

Table 1 – XRF analyses (1-7: bulk compositions) and selected EDS analyses (8-19: interstitial glass) of the lavas, scorias and pumices erupted at Stromboli volcano during the 2002-2003 volcanic activity.

Sample	St55	St61	St603	St51	St59	St62	St64	St53	St53
Type	Lava[a]	Lava[a]	Lava[a]	Scoria[b]	Scoria[b]	Pumice[c]	Pumice[c]	Lava[a]	Lava[a]
Analysis #	1	2	3	4	5	6	7	8	9
Date	Dec 02	Feb 03	Jun 03	Jun 02	Dec 02	Apr 03	Apr 03	Dec 02	Dec 02
SiO_2	49.7	49.6	49.6	49.9	49.9	48.6	49.3	51.7	52.1
TiO_2	0.91	0.93	0.92	0.81	0.88	0.91	0.88	1.64	1.59
Al_2O_3	17.1	17.1	17.3	17.2	16.6	17.2	17.3	15.1	15.4
Fe_2O_3*	8.86	8.71	8.76	8.67	8.94	8.70	8.93	9.40	9.49
MnO	0.16	0.16	0.16	0.16	0.16	0.16	0.16	n.d.	n.d.
MgO	6.27	6.04	6.13	6.46	6.74	6.13	6.49	3.65	3.56
CaO	11.3	11.2	11.3	11.5	11.7	11.6	11.7	7.65	7.49
Na_2O	2.46	2.49	2.46	2.68	2.71	2.37	2.66	3.31	3.24
K_2O	2.12	2.16	2.10	1.88	2.06	1.91	1.82	4.52	4.29
P_2O_5	0.53	0.55	0.54	0.43	0.48	0.53	0.49	1.10	1.13
LOI**	0.10	0.12	-	0.12	-	0.14	0.09		
Total	99.5	99.1	99.2	99.8	100.2	98.3	99.9	98.1	98.3

Sample	St53	St53	St55	St55	St62	St62	St62	St62	St64	St64
Type	Lava[a]	Lava[a]	Lava[a]	Lava[a]	Pumice[c]	Pumice[c]	Pumice[c]	Pumice[c]	Pumice[c]	Pumice[c]
Analysis #	10	11	12	13	14	15	16	17	18	19
Date	Dec 02	Dec 02	Jan 03	Jan 03	Apr 03	Apr 03	Apr 03	Apr 03	Apr 03	Apr 03
SiO_2	52.1	51.6	50.3	50.9	49.3	49.7	48.5	49.2	48.0	48.1
TiO_2	1.44	1.80	1.32	1.78	1.07	1.06	0.96	1.02	0.98	1.14
Al_2O_3	15.2	15.3	18.2	15.2	17.8	17.8	17.6	17.7	16.98	17.12
Fe_2O_3*	9.29	10.66	8.23	11.2	8.63	7.96	8.74	7.43	8.20	9.31
MnO	n.d.	0.12	0.10	n.d.	n.d.	0.10	n.d.	n.d.	n.d.	n.d.
MgO	3.62	2.93	2.45	3.22	5.39	5.08	5.98	6.03	5.83	5.98
CaO	7.36	7.56	9.09	5.68	13.3	12.1	12.5	13.6	12.1	11.9
Na_2O	3.06	3.13	3.52	3.35	2.29	2.26	2.15	2.15	2.5	2.4
K_2O	4.24	4.46	3.39	5.13	1.57	2.53	1.91	1.38	2.1	2.5
P_2O_5	1.20	1.28	1.17	1.33	n.d.	0.93	0.57	0.88	0.78	0.68
Total	97.5	98.8	97.7	97.8	99.3	99.5	98.9	99.3	97.4	99.2

* - total iron as Fe_2O_3; ** Loss on ignition;
a - sampled along the Sciara del Fuoco;
b - sampled near and below the crater area;
c - sampled in the summit area;
n.d. - not detected

Arenal volcano is a relatively small stratovolcano of Costa Rica tha resumed its activity in 1968 and is currently one of the most active in the world (Simkin and Siebert, 2000). It is about 1720 m above the sea level. It lies along a volcanic chain that has migrated to the NW from the late-Pleistocene Los Perdidos lava domes through the Pleistocene-to-Holocene Chato volcano. After several centuries of quiescence, Arenal volcano has been erupting almost continuously since September 1968. This activity started with a lateral blast eruption which occurred in July 1968, opened three new craters and reactivated one (Alvarado *et al.*, 2006). With the exception of the major explosion of June 1975, that produced a pyroclastic flow, the activity of Arenal was dominated by lava flows until 1984, when it entered its current and more explosive phase, characterised by strombolian eruptions, blocky lava flows, lava avalanches and pyroclastic flows. At the summit, a permanent "lava-pool" within the crater area overflows the crater rim producing continuous lava flows that descend the volcano's flanks.

The Arenal juvenile materials which have been studied in this work are associated to pyroclastic flows occurred in 1975, 1993, 1998, 2000 and 2001 years. They are essentially bombs and lapilli of basaltic andesites which exhibit a porphyritic to glomeroporphyritic texture with phenocrysts of calcic plagioclase (bytownite-labradorite), hypersthene, augite, and titaniferous magnetite in a hyalopilitic to pilotaxitic matrix consisting of intermediate plagioclase, hypersthene, augite, Ti-magnetite and interstitial glass (of dacitic composition). Apatite and zircon are accessory phases. The interstital glass is uniformely distributed in all thin sections, occasionally it is found in pools surrounding the vesicles. Xenocrysts of anorthite (~ An_{90}, with rims of labradorite) are locally present, whereas xenocrystic olivine crystals are sporadic and they are compositionally and texturally identical to those found in the lavas (Table 2).

Table 2 – XRF analyses (1-5: bulk compositions) and selected EDS analyses (6-10: interstitial glass) of the juvenile products associated to pyroclastic flows erupted at Arenal between 1975 and 2001 years.

Sample	Are75	Are93	Are98	Are00	Are01	Are75	Are00	Are98	Are93	Are01
Type*	b&b	b&b	b	b	b&b	b&b	b	b	b&b	b&b
Analysis #	1	2	3	4	5	6	7	8	9	10
Date	Jun 75	Aug 93	May 98	Aug 00	Mar 01	Jun 75	Aug 00	May 98	Aug 93	Mar 01
SiO_2	53.6	55.4	54.3	55.1	53.6	64.5	66.6	66.3	64.3	67.1
TiO_2	0.60	0.62	0.58	0.61	0.60	1.09	0.93	1.11	0.99	1.01
Al_2O_3	18.5	19.1	18.9	18.6	17.9	14.2	13.8	13.7	14.4	13.9
Fe_2O_3**	7.82	7.87	7.25	7.93	7.80	7.18	6.14	6.91	6.56	6.35
MnO	0.15	0.15	0.14	0.15	0.15	0.43	0.48	0.19	0.41	0.58
MgO	4.66	4.39	3.86	4.59	4.48	1.75	1.48	1.63	1.42	1.24
CaO	9.3	8.8	8.7	8.8	8.2	5.20	4.30	4.86	5.27	4.53
Na_2O	2.86	3.12	3.07	3.07	2.96	4.29	4.38	4.17	4.40	3.73
K_2O	0.58	0.68	0.65	0.67	0.66	1.66	1.83	1.88	1.50	1.92
P_2O_5	0.16	0.18	0.17	0.17	0.17	0.64	0.59	0.63	0.61	0.59
Cr_2O_3	0.01	0.01	0.00	0.01	0.01					
LOI***	1.17	-	2.01	-	3.48					
Total	99.5	100.2	99.6	99.5	100.0	100.9	100.5	101.4	99.8	100.9

* b = bomb, b&b = bomb and block; ** - total iron as Fe_2O_3, *** - Loss on ignition.

CRYSTAL SIZE DISTRIBUTION

An accurate estimate of the crystal content has been obtained applying image analysis to both optic microscope and SEM pictures, thus constraining crystal size distribution plots. The CSD gives insights on the kinetics and dynamics of crystallization (Marsh, 1988; Cashman & Marsh, 1988; Armienti *et al.*, 1994) by means of quantitative analyses of rock textures, which provide information on both the rate of crystallization and on the path through which those processes occurred.

Three-dimensional size distributions were obtained by calculating an average length of each crystal per size class (L) using the square root of individual crystal area measurement. I then calculated areal number densities for each size class (N_{Ac}), and converted them into a three-dimensional distribution (number per unit volume, N_{Vc}) according to Cashman & McConnell (2005):

$$N_{V_C} = \frac{N_{A_C}}{L} \qquad 1$$

This procedure has been shown to be a reliable method to correct the "intersection probability" since designated sampling planes are proportional to crystal size (Underwood, 1970). Following Randolph & Larson (1971), the obtained N_{Vc} data may be easily converted to crystal size distributions (CSDs) for the selected samples. For steady conditions of crystal nucleation and growth (Cashman, 1990):

$$n = n^o \exp\left(\frac{L}{L_d}\right) \qquad 2$$

where n^o is the crystal number density and L_d is the number-referenced dominant size. If data are linearly distributed, the plot *Ln(N_v) vs. L (mm)* will yield a straight line with a slope of *-1/L_d* and intercept n^o. The total number of crystals per unit volume can be calculated as $N_t = n^o L_d$. Assuming that the dominant size is a consequence of steady growth *(G)* over a certain period of time *(τ)*, we can say that $L_d = G\tau$ and, as a consequence, I could be able to estimate the residence time of crystals in the three different intervals of crystallization.

CSD plots (Fig. 1 and 2) show that data are uniform and linearly distributed, thus, assuming a steady growth over a certain period of time I was able to estimate the residence time of magma in the subvolcanic regions. This has been achieved by applying different growth rates related to the interval of crystallization (Armienti *et al.*, 2007), which takes into account the resorption effects in the magma chamber. Conversely, I used the growth rate of Kirkpatrik (1977) in the case of pumice microlites, which has been shown to be consistent with the experimental data obtained during the current research. Results give a range of residence times which are somehow similar for both volcanoes.

Using Armienti *et al.*'s (2007) *balanced growth rate* of 10^{-9} mm/sec, Stromboli scoria and recent lava phenocrysts with L > 0.80 mm live in the magma chamber between 6 and 11 years; Arenal phenocrysts residence times range from 5-7 years (collapses-type juveniles, L > 0.20 mm) and 9-12 year (explosion-type juveniles, L > 0.80 mm). Phenocrysts of both Stromboli (scoria and recent lavas, crystals with L < 0.80 mm) and Arenal products (explosion-type juvenile ejecta with L < 0.80 mm and collapses-type juveniles with L < 0.20 mm) result to be ~ 3 years.

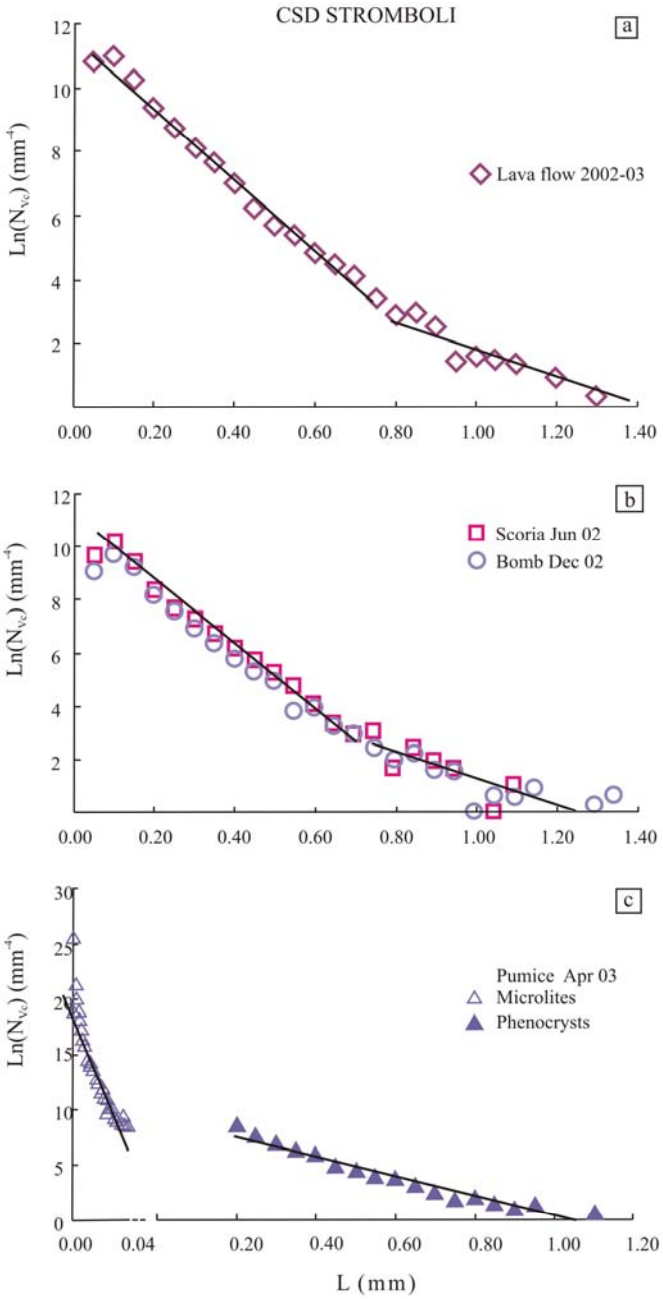

Fig. 1 – Crystal Size Distribution (CSD) plots for each products of the Stromboli eruptive crisis. (a) Crystals of the 2002-2003 lava flows. (b) Scoria and bomb sampled in June and December 2002 respectively. (c) Microlites (open triangles) and phenocrysts (closed triangles) of the 5th April 2003 golden pumice. In (c) the data gap is due to the different image acquisitions: in the case of microlites images were collected by means of SEM, while for phenocrysts images were acquired at optical microscope. Data distributions are well described by the straight lines.

For the Stromboli "golden pumice" ejected on April 5, 2003, I applied Kirkpatrik's (1977) growth rate ($3.8 \cdot 10^{-7}$ mm/s) on the microlites widely dispersed in the interstitial melt (images collected by SEM). In this case the residence time is only two hours. This is consistent with the dynamics of paroxysmal eruption.

Based on average bubble distances, the estimated times for the exsolution of the gaseous phases range from 2-7 days (assuming the gas phase to be predominantly CO_2,) to 44 minutes (in case of water only) for Stromboli lavas and scorias, down to about 15 hours to 12 minutes for the pumices erupted

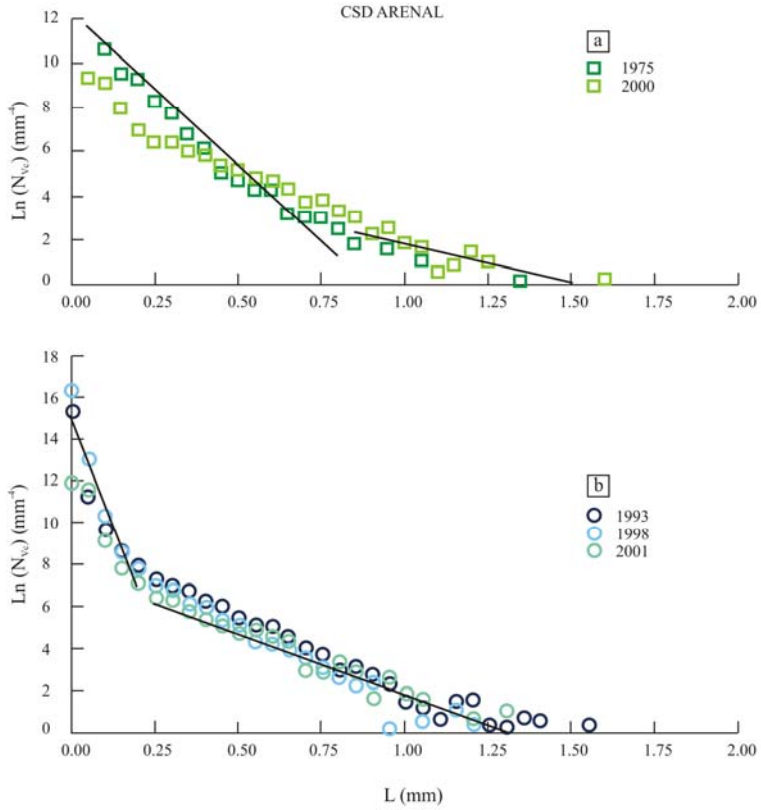

Fig. 2 – Crystal Size Distribution (CSD) plots for Arenal products. (a) Pyroclastic flows generated by energetic explosions occurred in 1975 and 2000. (b) Pyroclastic flows due to due to (partial) collapses of the lava-pool and/or lava-front occurred in 1993, 1998 and 2001. Data are well described by the straight lines.

during paroxysmal explosions. In the case of Arenal ejecta, the time of exsolution of the volatile content ranges between 4 and 6 hours. These results suggest that during the onset of major eruption, responsible for the emplacements of pyroclastic flows at Arenal volcano, the magma likely rose rapidly but was allowed to release very efficiently the gaseous phases and this process did not lead to a major explosion.

VISCOSITY MEASUREMENTS ON SILICATE MELTS

To establish a viscosity model applicable to various geological situations, the melt viscosity must be known over a wide range of temperatures. Experimental data can be obtained at high temperatures above the liquidus ($\eta < 10^6$ Pa s) and at low temperatures near the glass transition ($\eta > 10^8$ Pa s). In the low viscosity range (0.1 to 10^6 Pa s) higher pressures are required to study melts containing volatiles and experiments and can be realized applying the falling sphere technique. The settling velocity of a high density sphere through a molten sample is determined from the initial and final position in a quench experiment. This velocity is used to solve the well known Stokes' law for viscosity:

$$\eta = \frac{2\,t\,g\left(\rho_{sphere} - \rho_{melt}\right)r^2}{9\,d}\,C_F \qquad 3$$

in which η in the viscosity, t is the run time, ρ_{sphere} is the sphere density, ρ_{melt} is the melt density, g is the acceleration due to gravity (9.81 m/s^2), r is the radius of the sphere, d is the distance covered by the Pt sphere and C_F is the Faxen correction to account for the retarding effect of the container walls on the sphere motion (also known as wall effect):

$$C_F = 1 - 2.104\left(\frac{r}{R}\right) + 2.09\left(\frac{r}{R}\right)^3 - 0.95\left(\frac{r}{R}\right)^5 \qquad 4$$

where *r* is the sphere radius and *R* is the inner radius of the capsule.

Two types of experiments have been performed: on hydrous and anhydrous melts with composition of Stromboli and Arenal erupted products.

I used $Au_{80}Pd_{20}$ capsules, talc-pyrex-MgO assemblies with straight graphite furnaces and B-type thermocouples to synthesize the starting hydrous glass, while for anhydrous starting material I used $Au_{50}Pd_{50}$ capsule in order to reach temperatures above the liquidus to have a homogeneous crystal- and bubble-free glass. For falling sphere experiments, I adopted the commonly used NaCl-pyrex-MgO assembly in order to have a more precise control on the pressure (5 kb) and both $Au_{80}Pd_{20}$ and $Ag_{25}Pd_{75}$ capsules, the latter alloy composition can be passed through X-ray, which means that not only it is not necessary to open the capsule, but also that it is possible to use the same glass multiple times unless the sphere reaches the bottom or cap of the capsule. X-ray images of the glasses have been analyzed with a proper software for picture and in some case segmented in order to detect the exact position of the sphere in the melt. The dwell time used in the hydrous experiments is ranging from a minimum of 103 seconds to a maximum of 900 seconds, for the second set (anhydrous experiments) it has been increased from a minimum of 5400 seconds to a maximum of 21600 seconds, resulting in a lower error.

Results indicate that the viscosity of hydrous melt at 1200ºC and 5 kb varies between $1.2 \cdot 10^1$ and $5.2 \cdot 10^1$ Pa s; at 1100ºC and 5 kb viscosity increases of one order of magnitude, ranging from $1.3 \cdot 10^2$ to $2.8 \cdot 10^2$ Pa s. Experiments performed on anhydrous glasses, at 1150ºC and 5 kb result in higher values ranging from $5.2 \cdot 10^3$ Pa s to $1.4 \cdot 10^4$ Pa s.

MODELLING VISCOSITY

To investigate the viscosity of the melt and erupted magma I used several modified Einstein-Roscoe equations. In order to have a realistic estimate of this parameter for the melt component (preserved as glass), I constructed a modified Tammann-Vogel-Fulcher (TVF) (Vogel, 1921; Fulcher, 1925; Tammann & Hesse, 1926) equation by integrating the model of Giordano & Dingwell (2003) (at low temperatures) with that of Shaw (1972) (at high temperatures) and included a term to take into account the water content within the melt:

$$\mathrm{Log}_{10}\eta = A_{TVF} + \frac{B_{TVF}}{T - T_0} - CX_w \qquad 5$$

where η is the viscosity of the melt (Pa s), T is the temperature (K) and A_{TVF}, B_{TVF} and T_0 are adjustable parameters known as the shift factor, the non-Arrhenian pseudo-activation energy, the TVF temperature, C is the additional parameter for the water content and X_w is the mole fraction of water in the silicate melt (Cigolini *et al.*, 2008) (Table 3).

At Stromboli, the viscosity of the silicate liquids was initially calculated as anhydrous, using equation (5) at three different temperatures (1200, 1150 and 1100ºC), and the results range from $1.6 \cdot 10^2$ and $6.2 \cdot 10^2$ Pa s (golden pumice) and from $4.0 \cdot 10^2$ to $1.6 \cdot 10^3$ Pa s (recent lavas). By applying the equation proposed by Pinkerton & Stevenson (1992), I then retrieved the viscosities considering the effect of the crystallinity of the rocks (0.07 for the golden pumice and 0.38 for recent lavas). As a consequence the

values rise by almost one order of magnitude, ranging from $2.0 \cdot 10^3$ to $7.6 \cdot 10^3$ Pa s (golden pumice) and from $8.0 \cdot 10^3$ to $3.1 \cdot 10^4$ Pa s (recent lavas), respectively. The latter values are consistent with the estimated viscosities based on field measurements on active lava flows made in March 2007 and February-March 2003 (C. Cigolini, unpublished data).

Table 3 – Parameters for the modified TVF equation (5) for Stromboli basalts (Lava 2003 and Pumice April 2003) and Arenal andesites (Explosions and Collapses).

Type	Lava 2003*	Pumice Apr 2003 **	Explosion ***		Collapse ****		
Sample	St53 / St55	St62 / St64	Are75	Are00	Are93	Are98	Are01
A_{TVF} [a]	-1.41(35)	-1.65(33)	-1.81(34)	-1.77(31)	-1.78(28)	-1.78(25)	-1.77(24)
B_{TVF} [b]	3137(301)	2975(273)	3107(313)	3191(298)	3219(271)	3247(251)	3280(239)
T_0 [c]	691(16)	703(14)	688(17)	680(16)	677(15)	675(14)	672(13)
C [d]	20(2)	19(2)	0.51(5)	0.53(5)	0.54(5)	0.54(5)	0.56(5)
R [e]	0.99	0.99	0.98	0.97	0.97	0.97	0.97

Standard deviation is given in brackets and refers to the last digit.
* average of analyses 8-13 in Table 1. ** average of analyses 14-19 in Table 1.
*** average of analyses 6-7 in Table 2. **** average of analyses 8-10 in Table 2.
[a] shift factor. [b] non-Arrhenian pseudo-activation energy. [c] TVF temperature.
[d] new adjustable parameter for the water content. [e] linear correlation coefficient.

The same approach has been applied to Arenal melt. Anhydrous melt viscosity ranges between $1.4 \cdot 10^2$ and $8.1 \cdot 10^2$ Pa s, while considering the crystallinity (0.42-0.54) effect values rise of two orders of magnitude ranging between $3.4 \cdot 10^3$ and $6.4 \cdot 10^4$ Pa s. Furthermore, the model has been tested on the significantly more crystallized lavas resulted from crystal nucleation and growth while cooling at or near the surface. In this case viscosity exhibits values of 10^6 Pa s which are consistent with field measurements of Cigolini *et al.* (1984).

CONCLUSIONS

Information about the kinetics and dynamics of crystallization was obtained through the Crystal Size Distribution. Applying this method I accurately estimated rocks crystallinities and inferred magma residence times from the crystallization of phenocrysts and microlites and results are in agreement with the plumbing system of the analyzed volcanoes.

The measurements of silicate melts viscosity through the "falling sphere" method gave new experimental data and results comparable with field measurements.

The new model (MOD-TVF) to calculate viscosity of the basaltic and andesitic melts takes into account the water content, gives good results on both low and high crystallinity rocks and is in good agreement with the experimental measurements. In the light of the above, the systematic use of MOD-TVF equation combined with the modified Einstein-Roscoe (MER) equations can overcome the discrepancies this far observed between field measurements and calculated viscosities.

REFERENCES

Alvarado, G.E., Soto, G.J., Schmincke, H.U., Bolge, L.L., Sumita, M. (2006): The 1968 andesitic lateral blast eruption at Arenal volcano, Costa Rica. *J. Volcanol. Geotherm. Res.*, **157**, 9-33.

Armienti, P., Francalanci, L., Landi, P. (2007): Textural effects of steady state behaviour of the Stromboli feeding system. *J. Volcanol. Geotherm. Res.*, **160**, 86-98.

Armienti, P., Pareschi, M.T., Innocenti, F., Pompilio, M. (1994): Effects of magma storage and ascent on the kinetics of crystal growth. The case of 1991-93 Mt. Etna eruption. *Contrib. Mineral. Petrol.*, **115**, 402-414.

Barberi, F., Rosi, M., Sodi, A. (1993): Volcanic hazard assessment at Stromboli based on review of historical data. *Acta Vulcanol.*, **3**, 173-187.

Cashman, K.V. & Marsh, B.D. (1988): Crystal size distribution (CSD) in rocks and the kinetics and dynamics of crystallization II: Makaopuhi lava lake. *Contrib. Mineral. Petrol.*, **99**, 292-305.

Cashman, K.V. & McConnell, S.M. (2005): Multiple levels of magma storage during the 1980 summer eruptions of Mount St. Helens, WA. *Bull. Volcanol.*, **68**, 57-75.

Cashman, K.V. (1990): Textural constrains on the kinetics of crystallization of igneous rocks. *In*: "Modern methods of igneous petrology: understanding magmatic processes", J. Nicholls & J.K. Russel, eds. *Rev. Mineral.*, **24**, 259-314.

Cigolini, C., Borgia, A., Casertano, C. (1984): Intracrateric activity, aa-block lava viscosity and flow dynamics: Arenal Volcano, Costa Rica. *J. Volcanol. Geotherm. Res.*, **20**, 155-176.

Cigolini, C., Laiolo, M., Bertolino, S. (2008): Probing Stromboli volcano from the mantle to paroxysmal eruptions. *In*: "Dynamics of crustal magma transfer, storage, and differentiation – Integrating geochemical and geophysical constraints", G. Zellmer & C. Annes, eds. *Geol. Soc. London Spec. Publ.*, in press.

Fulcher, G.S. (1925): Analysis of recent measurements of the viscosity of glasses. *J. Am. Cer. Soc.*, **8**, 339-355.

Giordano, D. & Dingwell, D.B. (2003): Non-Arrhenian multicomponent melt viscosity: a model. *Earth Planet. Sci. Letters*, **208**, 337-349.

Kirkpatrik, R.J. (1977): Nucleation and growth of plagioclase, Makaopuhi and Alae lava lakes, Kilauea Volcano, Hawaii. *Geol. Soc. Am. Bull.*, **88**, 78-84.

Marsh, B.D. (1988): Crystal size distribution (CSD) in rocks and the kinetics and dynamics of crystallization I: Theory. *Contrib. Mineral. Petrol.*, **99**, 277-291.

Newhall, C. & Self, S. (1982): The volcanic explosivity index (VEI) – an estimate of explosivemagnitude for hystorical volcanism. *J. Volcanol. Geotherm. Res.*, **87**, 1231-1238.

Pinkerton, H. & Stevenson, R.J. (1992): Methods of determining the rheological properties of magmas at sub-liquidus temperatures. *J. Volcanol. Geotherm. Res.*, **53**, 47-76.

Randolph, A.D. & Larson, M.A. (1971): Theory of particule processes. Academic Press, New York, 251 p.

Shaw, H.R. (1972): Viscosity of magmatic liquids: an empirical method of prediction. *Am. J. Sci.*, **272**, 870-893.

Simkin, T. & Siebert, L. (2000): Volcanoes of the world. Geoscience Press, Tucson, 349 p.

Tammann, G. & Hesse, W. (1926): Die Abhängigkeit der Viskosität von der temperatur bei unterkhülten Flüssigkeiten, *Z. Anorg. Allgem. Chem.*, **156**, 245-257.

Underwood, E.E. (1970): Quantitative stereology. Addison-Wesley, Reading, 274 p.

Vogel, D.H. (1921): Temperaturabhängigkeitsgesetz der Viskosität von Flüssigkeiten. *Z. Phys. Chem.*, **22**, 645-646.